

Lacunarity for Spatial Heterogeneity Measurement in GIS

Pinliang Dong

Department of Geology, University of New Brunswick
Fredericton, New Brunswick Canada E3B 5A3

Abstract

As a scale dependent measure of heterogeneity, lacunarity has been applied to the analysis of structures in both fractals and non-fractals. In this paper, the lacunarity concept and some lacunarity estimation methods are briefly described, then a Lacunarity Analysis extension for ArcView GIS (ESRI) is introduced. Using binary and gray-scale images, several examples are also given for lacunarity analysis of spatial heterogeneity. Experiments with gray-scale image textures show that a new lacunarity estimation method can provide more accurate heterogeneity measurement than some existing methods. The results suggest that lacunarity analysis is a promising tool for spatial heterogeneity measurement in a GIS environment.

I. INTRODUCTION

Spatial heterogeneity exists in both natural and human-dominated phenomena, and affects many processes on this planet. For example, spatial heterogeneity associated with soil properties, land cover, and localized precipitation influences soil moisture and surface fluxes [1]. Spatial heterogeneity also affects the use of remote sensing measurements at various resolutions for deriving surface parameters such as Leaf Area Index (LAI), and for estimating processes such as gas and energy exchange between the surface and the atmosphere [2]. In landscape ecology, the effects of spatial pattern on ecological processes is a key problem area [3], and coexistence through spatial heterogeneity has been shown for both animals [4] and plants [5]. In addition, spatial heterogeneity varies at different scales, and scaling has been recognized as one of the most important and pressing challenges across all fields of Earth sciences [6-10]. To better understand the pattern of spatial heterogeneity, the effects of changing scale must be taken into account.

Lacunarity is introduced by Mandelbrot [11] to describe the characteristic of fractals of the same dimension with different texture appearances. The lacunarity concept has been extended to any set that is not necessarily fractal at any arbitrary scale [12], which allows for application of lacunarity to both fractals and non-fractals. In fact, many natural objects are fractal only in a limited scale range rather than in the full scale range [13][14].

Spatial heterogeneity is one of the questions standing in the way of confirmatory spatial data analysis. Over the years, much emphasis has been put on the modeling capabilities of geographic information

systems (GIS) so that that their full potential as an analytical tool is realized. Increasingly, the measurement of spatial heterogeneity and effects of scaling have become important issues in geographical information science. In a previous paper [15], the author proposed a new method for lacunarity estimation with gray-scale images. In this paper, the lacunarity concept and some lacunarity estimation methods are introduced, then the development of a Lacunarity Analysis extension for ArcView GIS (ESRI) is presented. Several examples are also given for lacunarity analysis of binary and gray-scale images. Finally, some aspects of lacunarity for heterogeneity measurement are discussed.

II. FRACTAL GEOMETRY AND LACUNARITY

Many natural objects are so complex and irregular that models of classical geometry are insufficient to describe them. Since the advent of Mandelbrot's work [11], fractal geometry has received increased attention as a novel model for natural phenomena. Many researchers attempted to use fractals in different fields such as sedimentology analysis [16], particle morphology description [17], computer graphics generation [18], geological structural analysis and geophysical data analysis [19][20], geomorphological surface study [21], and spatial statistics [22]. Generally, the application of fractal geometry has led to a far greater understanding of fundamental processes in physics and chemistry which influence many other fields [23][24].

Fractal dimension can be viewed as a measure of irregularity of many physical processes. There has

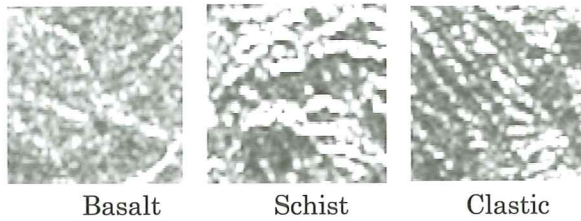


Figure 1. Sample images of three rock units (79 x 79 pixels each) from a Shuttle Imaging Radar (SIR-C) imagery (L-band HH-polarization) near Yuma, Arizona, USA. Pixel size is 12.5 by 12.5 meters.

been increasing interest in the use of fractal dimension for spatial heterogeneity modeling in computer vision and pattern recognition [13][14][25-27]. In areas of remote sensing applications, a number of studies have been carried out to evaluate the usefulness of fractal dimension for analysis of remotely sensed images of land surfaces [28-34]. However, different fractal sets may share the same fractal dimension and have strikingly different textures [11][35], just like visually different images may have the same gray-level histogram. As an example, Figure 1 shows three images of rock units extracted from a Shuttle Imaging Radar (SIR-C) imagery (L-band HH-polarization) near Yuma, Arizona, USA. Using a differential box counting method for fractal dimension estimation proposed by Sarkar and Chaudhuri [26], the fractal dimension values for the three sample images are 2.49, 2.48, and 2.49, respectively.

It can be seen that the fractal dimension of the three rock unit images can be very similar, even though they have different texture appearances. For discriminating these textures, fractal dimension alone would be useless. Mandelbrot [11] introduced the term lacunarity, from Latin *lacuna* for gap, to describe the characteristic of fractals of the same dimension with different texture appearances.

Lacunarity measures the deviation of a geometric object, such as a fractal, from translational invariance [36]. A geometric object is translationally invariant if different parts of the object are the same. Lacunarity is related to the distribution of gap sizes in a geometric object: homogeneous geometric objects have low lacunarity because all gap sizes are the same or almost the same, whereas heterogeneous objects have high lacunarity because gap sizes are quite different. At a given scale, lacunarity represents how similar are parts from different regions of a geometric object to each other. It should be noted that objects which are homogeneous at small scale can be quite heterogeneous when examined at larger scale and vice versa. Therefore, lacunarity can be considered a scale dependent measure of heterogeneity or texture [36].

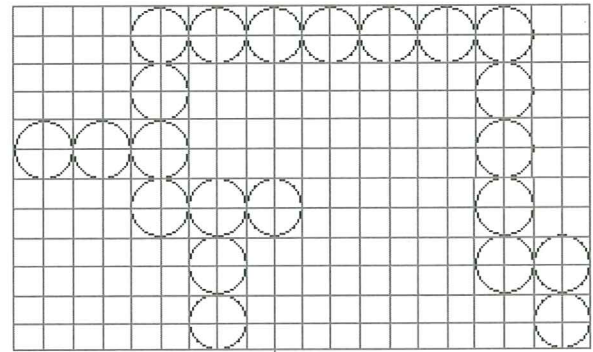


Figure 2. Illustration of the gliding-box method. The mesh size of the underlying lattice and the radius of a particle are $2a$ and ϵ , respectively. The gliding-box is a square of side $2r$, which is a multiple of $2a$. (Adapted from Allain and Cloitre [12])

III. METHODS OF LACUNARITY ESTIMATION

Methods for calculating lacunarity were given by Mandelbrot [11], Gefen *et al.* [37], and Lin and Yang [38]. Allain and Cloitre [12] found that most of the methods impractical or difficult to characterize a wide range of structures. Following a general approach which consists of analyzing the mass distribution in a deterministic or a random set, Allain and Cloitre [12] proposed a gliding-box algorithm of defining the lacunarity of the set. The gliding-box algorithm has been used for lacunarity analysis of binary images [39-42]. The algorithm is briefly introduced below.

Lacunarity of Binary Images – Gliding-box Algorithm

In the gliding-box algorithm, the set under study is placed on an underlying lattice with a mesh size equal to $2a$ (Figure 2). a is lower or equal to particle radius ϵ .

Now consider a box of radius r which “glides” on this lattice in all the possible manners, with its center being placed successively on the different sites of the underlying lattice. Let us define $n(M, r)$ to be the number of gliding boxes with radius r and mass M . The probability function $Q(M, r)$ is obtained by dividing $n(M, r)$ by the total number of boxes. It is convenient to analyze the properties of probability function $Q(M, r)$ starting from its statistical moments $Z_Q^{(q)}(r)$:

$$Z_Q^{(q)}(r) = \sum_M M^q Q(M, r) \quad (1)$$

The lacunarity at scale r is defined by the mean-square deviation of the fluctuations of mass distribution probability $Q(M, r)$ divided by its square mean:

$$\Lambda(r) = \frac{Z_Q^{(2)}(r)}{[Z_Q^{(1)}(r)]^2} = \frac{\sum_M M^2 Q(M, r)}{[\sum_M M Q(M, r)]^2} \quad (2)$$

The definition for lacunarity (equation 2) is general since it can be applied to any set which is not necessarily fractal at any arbitrary scale r .

Plotnick *et al.* [39][40] extended the concept of lacunarity and the gliding-box algorithm to the description of spatial distribution of real data sets, including, but not restricted to, fractal and multifractal distributions. Based on a random binary map which has two values (0 for empty and 1 for occupied), they extended equation 2 as:

$$\Lambda(r) = \frac{S_s^2(r)}{\bar{S}^2(r)} + 1 \quad (3)$$

where $\bar{S}(r)$ is the mean and $S_s^2(r)$ the variance of the number of the occupied sites at scale r (i.e., gliding-box size $r \times r$).

Lacunarity of Gray-scale Images

Spatial data sources for a geographic information system may have a three-dimensional structure, i.e., x and y coordinates and z values. For example, digital elevation models (DEM), population density maps, and remotely sensed images all have x , y , and z values and can be displayed as gray-scale images. Gray-scale images can be converted into binary quartiles [41][42], then lacunarity indices can be derived from the binary quartiles using the gliding-box algorithm. However, information on the spatial heterogeneity of a binary quartile may not reflect the spatial heterogeneity of the original gray-scale image due to the loss of spatial information during conversion from gray-scale (for example 8-bit) to binary (1-bit). It is therefore essential to obtain lacunarity of a gray-scale image directly.

Voss [35] proposed a probability method to estimate the fractal dimension and lacunarity of image intensity surfaces. Let $P(m, L)$ be the probability that there are m intensity points within a box of size L centered about an arbitrary point of image intensity surface, we have

$$\sum_{i=1}^N P(m, L) = 1 \quad (4)$$

where N is the number of possible points in the box of L . Letting

$$M(L) = \sum_{m=1}^N m P(m, L) \quad (5)$$

and

$$M^2(L) = \sum_{m=1}^N m^2 P(m, L) \quad (6)$$

the lacunarity is defined as

$$\Lambda(L) = \frac{M^2(L) - (M(L))^2}{(M(L))^2} \quad (7)$$

In an earlier paper, the author proposed a new method of lacunarity estimation for gray-scale images [15]. The method was based on the differential box counting method proposed by Sarkar and Chaudhuri [26], and the gliding-box algorithm [12]. Comparisons of the new method and the method by Voss [35] can be found in Section 5 of this paper.

IV. IMPLEMENTATION OF LACUNARITY ANALYSIS IN GIS

A Lacunarity Analysis extension for ArcView GIS (ESRI) is developed using the Dialog Designer and Avenue scripting language of ArcView GIS and the C

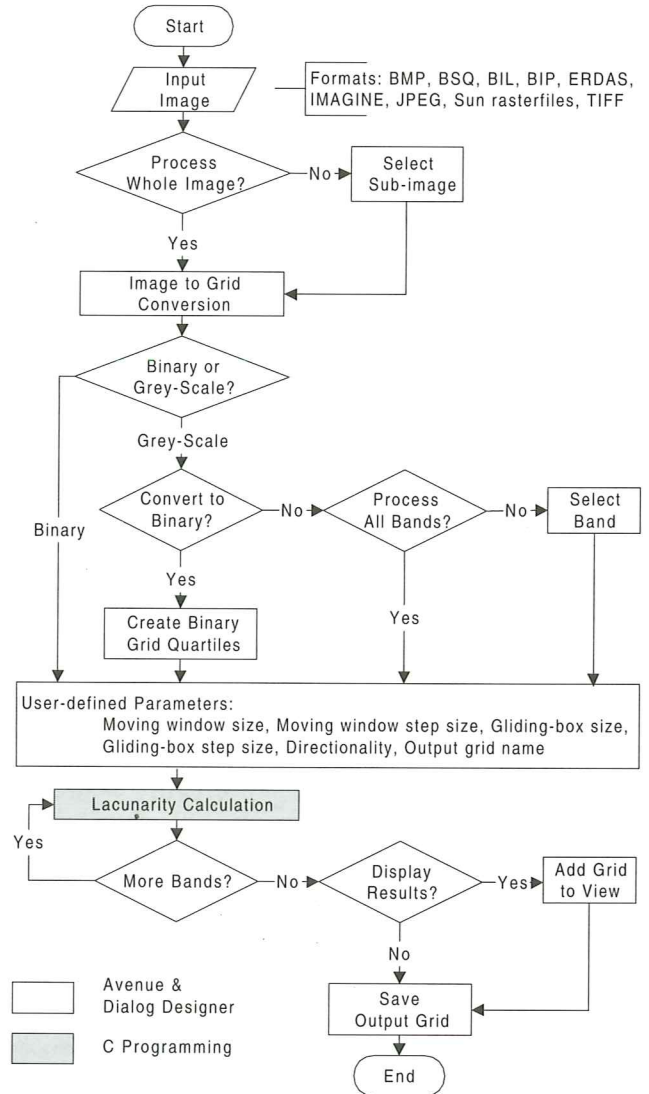


Figure 3. Flow chart for the Lacunarity Analysis extension

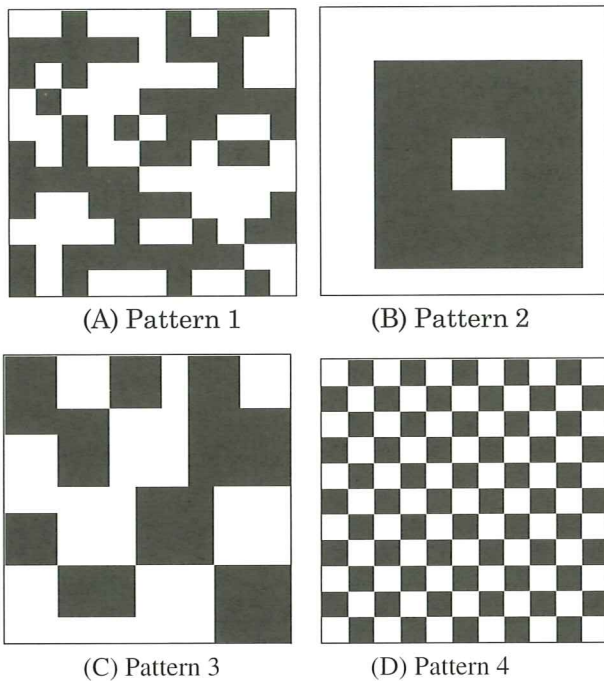


Figure 4. Binary images of the four spatial patterns

programming language. The Dialog Designer and Avenue provide tools for developing a Graphical User Interface (GUI), while the C programming language implements calculation of lacunarity in the moving windows across the input image, which is relatively intensive in computation. For lacunarity estimation of binary images, the gliding-box algorithm proposed by Allain and Cloitre [12] was used. For gray-scale images, a new method based on differential box counting and gliding-box algorithm was employed [15]. The design of the Lacunarity Analysis extension is shown in Figure 3. The output results from lacunarity analysis are in ESRI GRID format, which allows for convenient integration of the results into other ArcView GIS extensions, such as Spatial Analyst and ModelBuilder (ESRI). In case the user selects the input image size as moving window size, the output is not a grid but rather a chart showing the lacunarity curve. The Lacunarity Analysis extension can be used on PCs with ESRI's ArcView GIS (version 3.0 or later) on Windows 95/98/NT (Microsoft) operating systems. With minor modifications, the extension can be used on other platforms.

V. EXAMPLES

Example 1: Binary spatial patterns

Figure 4 shows four 11 x 11 binary image patterns, with white pixels representing 1's, and black pixels representing 0's. There are 61 white pixels and 60 black pixels for all four patterns. The lacunarity

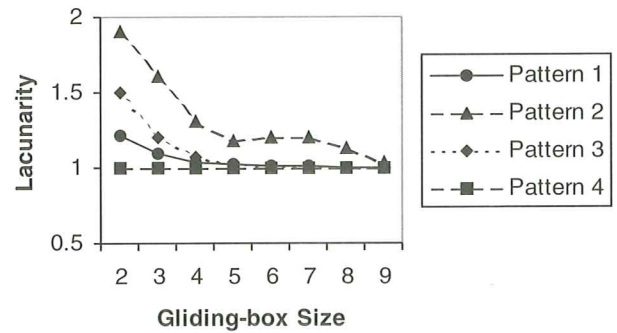


Figure 5. Lacunarity curves of the patterns shown in Figure 4.

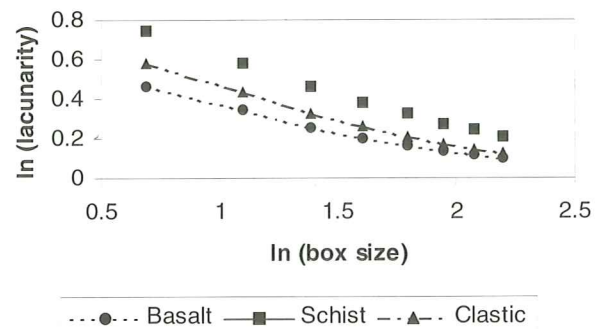


Figure 6. Lacunarity curves of the rock unit images shown in Figure 1.

measurements at scales $r = 2, 3, 4, 5, 6, 7, 8,$ and 9 are obtained for each pattern (Figure 5). It can be seen that lacunarity measure does reflect the geometry structure of the patterns. For example, pattern 2 (Figure 4B) has larger gaps than other patterns, and lacunarity is larger than that of the other three patterns due to the increase in fully occupied and totally empty boxes. In contrast, pattern 4 (Figure 4D) is a totally regular (i.e., translationally invariant) image, and the lacunarity is equal to 1 or very close to 1 because the number of occupied squares would be almost constant at any location.

Example 2: Sample images of rock units

Now let's go back to the three rock unit sample images (Figure 1) presented in Section 2 of this paper. Although they cannot be differentiated from each other using fractal dimension, their lacunarity curves are able to show their differences when the gliding-box size changes from 2 to 9 (Figure 6).

Example 3: Brodatz textures

Image texture is also a reflection of spatial heterogeneity. Figure 7A shows a mosaic of four texture images taken from Brodatz's album [43]. The size of texture image mosaic is 400 by 400 pixels. The texture image in the upper-left part of the mosaic is

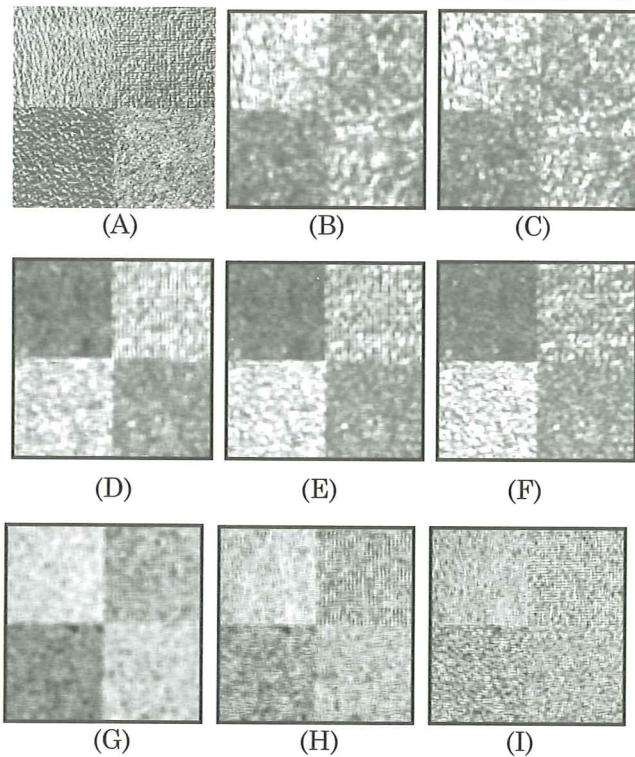


Figure 7. Comparison of lacunarity images. (A) Original texture image (400 x 400); (B) and (C) are lacunarity images derived from the second quartile binary image of (A) at $r = 3$ and 5 respectively; (D), (E), and (F) are lacunarity images obtained using the new method [15] at $r = 3, 5,$ and 7 respectively; (G), (H), and (I) are lacunarity images obtained using the Voss method [35] at $r = 3, 5,$ and 7 respectively. The moving window size is 15×15 . r – gliding-box size.

referred to as Texture 1, the upper-right as Texture 2, the lower-left as Texture 3, and the lower-right as Texture 4. Some result images from different lacunarity estimation methods are also shown in Figure 7. The lacunarity curves for the four textures are shown in Figure 8 with gliding-box size changing from 2 to 9.

Figure 8 shows that the lacunarity curve of Texture 3 has a slower decay rate than that of the other textures, and Texture 2 has higher lacunarity than Texture 3 when the gliding-box size (observation scale) $r = 2$. At $r = 3$, Texture 2 and Texture 3 have similar lacunarity. With the increase of gliding-box size, the lacunarity of Texture 3 is higher than that of Texture 2, and the differences in the lacunarity values increase, as shown also in the lacunarity images (Figure 7E, F). The example suggests that two textures may be differentiated at certain scales, even though they cannot be differentiated at some other scales.

Using maximum likelihood classification, the result

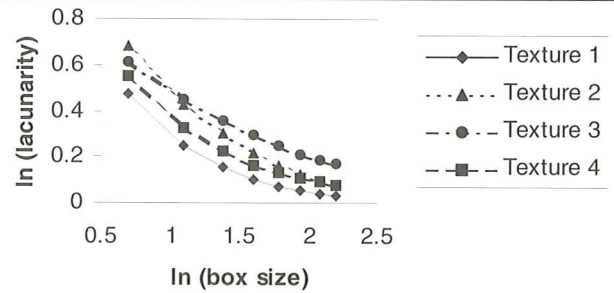


Figure 8. Lacunarity curves for the four textures shown in Figure 7A (gliding-box size $r = 2, 3, 4, 5, 6, 7, 8, 9$).

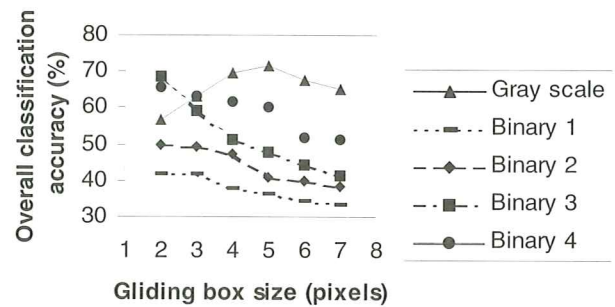


Figure 9. Comparison of overall classification accuracy between lacunarity images generated from gray-scale image using the new method [15] and quartile binary images at different scales. Binary 1 represents the first quartile binary image.

images from the new lacunarity measure [15] are compared with those from the quartile binary images derived from the gray-scale image (a method used in [41] and [42]), and with the lacunarity measure proposed by Voss [35]. Approximately 60 by 60 pixels for each texture category are used as training sites, and 1024 random points are used for classification accuracy assessment of each resultant image. The texture measurements are obtained using a 15 by 15 moving window for all the methods compared. It can be seen that the lacunarity measures for gray-scale image using the new estimation method in [15] can generate more accurate classification accuracy than lacunarity measures of the binary images, particularly when the gliding-box size is larger than 2 (Figure 9). When lacunarity images at different scales are combined for classification, the method in [15] also provide more accurate classification accuracy than the method due to Voss [35] and gliding-box method for binary images (Figure 10).

VI. CONCLUSIONS AND DISCUSSIONS

It has been shown in this paper that lacunarity can be used for the analysis of spatial heterogeneity at

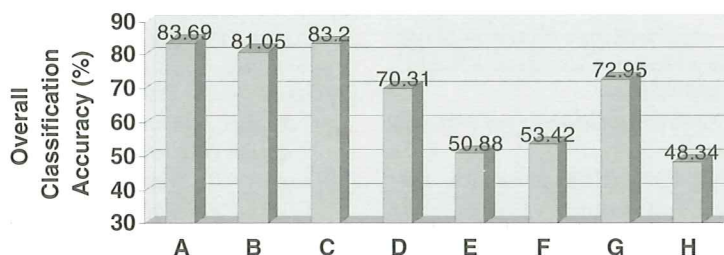


Figure 10. Comparison of overall classification accuracy for combined lacunarity images generated using different methods at different scales. A, B, and C are results from the new lacunarity estimation method [15] for gray-scale images. A – scales $r = 2, 3, 4, 5, 6, 7, 8,$ and 9 combined; B – scales $r = 3, 5,$ and 7 combined; C – scale $r = 3$ combined with lacunarity measures at directions 45° and 135° of the scale $r = 3$; D – result from the method by Voss [35] for scales $r = 3, 5,$ and 7 combined. E, F, G, and H are results from the 1st, the 2nd, the 3rd, and the 4th quartile binary images for scales r

different scales. For gray-scale images in which texture is an expression of spatial heterogeneity, a new lacunarity estimation method [15] has been proved to provide more accurate measurements for spatial heterogeneity than the method proposed by Voss [35] and the methods based on binary images [41][42]. This can be attributed to the ability of the new method that gives a better approximation to the image intensity surface.

Texture of an image (binary or gray-scale) exhibits the degree of spatial heterogeneity. Indeed, texture is a very important spatial characteristic in an image. Before introducing the lacunarity concept in his book, Mandelbrot [11] commented that: “Texture is an elusive notion which mathematicians and scientists tend to avoid because they cannot grasp it. Engineers and artists cannot avoid it, but mostly fail to handle it to their satisfaction.” It is reasonable to expect that spatial heterogeneity can be better understood by revealing several individual facets of image texture through lacunarity analysis.

Implemented in a GIS environment, lacunarity analysis provides a useful and convenient approach to spatial heterogeneity measurement. Unlike other studies where lacunarity analysis results are usually expressed as interpretable graphics [39-42], this paper shows that output from lacunarity can be in raster format in addition to graphics, which enables the integration of lacunarity analysis with other spatial modeling functions in a GIS. In this paper, lacunarity analysis is demonstrated on binary and gray-scale sample images. It is desirable in the future to use real dataset, such as remotely sensed images and other raster data, to further explore the use of lacunarity as a scale dependent measure for spatial heterogeneity.

ACKNOWLEDGMENTS

The author would like to thank Drs. Paul Williams and Brigitte Leblon for their encouragement and support. Thanks are also due to my current employer BTG Inc./Delta Research Division for providing some of the research facilities, and to USGS EROS Data Center for providing the Shuttle Imagine Radar (SIR-C) data.

REFERENCES

- [1] Mölders, N. and Raabe, A., 1996, Numerical investigations on the influence of subgrid-scale surface heterogeneity on evapotranspiration and cloud processes, *Journal of Applied Meteorology*, 35: 782
- [2] Chen, J.M., 1999, Spatial Scaling of a Remotely Sensed Surface Parameter by Contexture, *Remote Sensing of Environment*, 69:30–42.
- [3] Turner, M.G. and Gardner, R.H., 1991, Quantitative methods in landscape ecology: An introduction. Turner, M.G. and Gardner, R.H. eds. Ecological Studies Series, Springer-Verlag, New York. *The Analysis and Interpretation of Landscape Heterogeneity*, 3-14.
- [4] Kareiva, P., 1986, Patchiness, dispersal, and species interactions: consequences for communities of herbivorous insects. Diamond, J. and Case, T.J. eds. Harper and Row, New York, *Community Ecology*, 192-206.
- [5] Pacala, S.W., 1987, Neighborhood models of plant population dynamics. III Models with spatial heterogeneity in the physical environment, *Theoretical Population Biology*, 31:359-392.
- [6] Levin, S.A., 1992, The problem of pattern and scale in ecology, *Ecology*, 73:1943-1967.
- [7] Qi, Y. and Wu, J., 1996, Effects of changing spatial scales on analysis of landscape patterns using spatial autocorrelation indices, *Landscape Ecology*, 11(1):39-49.
- [8] Van Gardingen, P. R., Foody, G.M. and Curran, P. J., 1997, *Scaling-Up: From Cell to Landscape*, Cambridge University Press, Cambridge.
- [9] Peterson, D. L. and Parker, V. T., 1998, *Ecological Scale: Theory and Applications*. Columbia University Press,

- New York.
- [10] Wu, J., 1999, Hierarchy and scaling: Extrapolating information along a scaling ladder, *Canadian Journal of Remote Sensing*, 25(4):367-380.
- [11] Mandelbrot, B.B., 1983, *The Fractal Geometry of Nature*, San Francisco, CA: Freeman.
- [12] Allain, C. and Cloitre, M., 1991, Characterizing the lacunarity of random and deterministic fractal sets, *Physics Review, A* 44: 3552-3558.
- [13] Pentland, A., 1984, Fractal-based description of natural scenes, *IEEE Transactions on Pattern Analysis and Machine Intelligence, PAMI-6*(6):661-674.
- [14] Peleg, S., Noar, J., Hartley, R., and Avnir, D., 1984, Multiple resolution texture analysis and classification, *IEEE Transactions on Pattern Analysis and Machine Intelligence, PAMI-6*(4):518-523.
- [15] Dong, P.L. Test of a new lacunarity estimation method for image texture analysis, *International Journal of Remote Sensing* (in press).
- [16] Orford, J.D. and Whalley, W.B., 1983, The use of fractal dimension to characterize irregular-shaped particle, *Sedimentology*, 30:655-668.
- [17] Kaye, B.H., 1986, Fractal dimension and signature wave form characterization of fine particle shape, *American Laboratory*, 55-63.
- [18] Kaandorp, J.A., 1987, Interactive generation of fractal objects, *Eurographics'87*, Elsevier Science Publishers B.V. North-Holland, 181-197.
- [19] Turcotte, D.L., 1989, Fractals in geology and geophysics, Scholz and Mandelbrot eds., *Fractals in Geophysics*, Birkhäuser Verlag Basel, 171-196.
- [20] Hirata, T., 1989, Fractal dimension of fault systems in Japan: Fractal structure in rock fracture geometry at various scales, in: Scholz and Mandelbrot eds., *Fractals in Geophysics*, Birkhäuser Verlag Basel, 157-170.
- [21] Snow, R.S. and Mayer, L. Eds., 1992, Fractals in Geomorphology, *Geomorphology*, 5(1/2):194.
- [22] Cheng, Q., 1999, Multifractality and spatial statistics, *Computers & Geosciences*, 25:949-961.
- [23] Stauffer, D. and Stanley, H.E., 1989, *From Newton to Mandelbrot: a primer in theoretical physics*: Springer Verlag, Berlin.
- [24] Harrison, A., 1995, *Fractals in chemistry*, New York: Oxford University Press, 90p.
- [25] Keller, J.M., Chen, S., and Crownover, R.M., 1989, Texture description and segmentation through fractal geometry, *Computer Vision, Graphics, and Image Processing*, 45:150-166.
- [26] Sarkar, N. and Chaudhuri, B.B., 1992, An efficient approach to estimate fractal dimension of textural images, *Pattern Recognition*, 25:1035-1041.
- [27] Huang, Q., Lorch, J.R., Dubes, R.C., 1994, Can the fractal Dimension of images be measured? *Pattern Recognition*, 27(3):339-349.
- [28] De Cola, L., 1989, Fractal analysis of a classified Landsat scene, *Photogrammetric Engineering and Remote Sensing*, 55(5):601-610.
- [29] Lam, N. S., 1990, Description and measurement of Landsat TM images using fractals, *Photogrammetric Engineering and Remote Sensing*, 56(2):187-195.
- [30] Jones, J.G., Thomas, R.W., and Earwicker, P.G., 1991, Multiresolution analysis of remotely sensed imagery, *International Journal of Remote Sensing*, 12(1):107-124.
- [31] Dellepiane, S., Giusto, D.D., Serpico, S.B., and Vernazza, G., 1991, SAR image recognition by integration of intensity and textural information, *International Journal of Remote Sensing*, 12(9):1915-1932.
- [32] Klinkenberg, B., 1994, A fractal analysis of shadowed and sunlit areas, *International Journal of Remote Sensing*, 15(5):967-977.
- [33] Roach, D. and Fung, K.B., 1994, Fractal-based textural descriptors for remotely sensed forestry data, *Canadian Journal of Remote Sensing*, 20(1):59-70.
- [34] Chen, K.S., Yen, S.K., and Tsay, D.W., 1997, Neural classification of SPOT imagery through integration of intensity and fractal information, *International Journal of Remote Sensing*, 18(4):763-783.
- [35] Voss, R., 1986, Random fractals: characterization and measurement, *Scaling Phenomena in Disordered Systems*, Pynn, R. and Skjeltorp, A. eds., Plenum, New York.
- [36] Gefen, Y., Meir, Y., and Aharony, A., 1983, Geometric implementation of hypercubic lattices with noninteger dimensionality by use of low lacunarity fractal lattices, *Physical Review Letters*, 50: 145-148.
- [37] Gefen, Y., Aharony, A., and Mandelbrot, B.B., 1984, Phase transitions on fractals: III. Infinitely ramified lattices, *Journal Physics A: Mathematical and General*, 17:1277-1289.
- [38] Lin, B., and Yang, Z.R., 1986, A suggested lacunarity expression for Sierpinski carpets, *Journal Physics A: Mathematical and General* 19: L49-L52.
- [39] Plotnick, R.E., Gardner, R.H., and O'Neill, R.V., 1993, Lacunarity indices as measures of landscape texture, *Landscape Ecology* 8(3):201-211.
- [40] Plotnick, R.E., Gardner, R.H., Hargrove, W.W., Prestegard, K., and Perlmutter, M., 1996, Lacunarity analysis: A general technique for the analysis of spatial patterns, *Physical Review E* 53(5):5461-5468.
- [41] Henebry, G.M., and Kux, H.J.H., 1995, Lacunarity as a texture measure for SAR imagery, *International Journal of Remote Sensing* 16(3):565-571.
- [42] Ranson, K.J., and Sun, G., 1997, An evaluation of AIRSAR and SIR-C/X-SAR images for mapping northern forest attributes in Maine, USA. *Remote Sensing of Environment*, 59:203-222.
- [43] Brodatz, 1966, *Texture: A photographic album for artists and designers*. Dover, New York.